AFRL-OSR-VA-TR-2013-0595

GEL SPUN PAN/CNT BASED CARBON FIBERS WITH HONEY-COMB CROSS-SECTION

SATISH KUMAR

GEORGIA TECH RESEARCH CORPORATION

11/13/2013
Final Report

AIR FORCE RESEARCH LABORATORY
AF OFFICE OF SCIENTIFIC RESEARCH (AFOSR)/RSA
ARLINGTON, VIRGINIA 22203
AIR FORCE MATERIEL COMMAND

REPORT DOCUMENTATION PAGE

Form Approved
OMB No. 0704-0188

PLEASE DO NOT RETURN YOUR FORM TO THE ABOVE ORGANIZATION.

1. REPORT DATE *(DD-MM-YYYY)*	2. REPORT TYPE	3. DATES COVERED *(From - To)*
06/11/2013	Final Technical Report	15/08/2010 - 14/08/2013

4. TITLE AND SUBTITLE
Gel spun PAN/CNT based carbon fibers with honey-comb cross-section

5a. CONTRACT NUMBER
FA9550-10-1-0475

5b. GRANT NUMBER

5c. PROGRAM ELEMENT NUMBER

6. AUTHOR(S)
Satish Kumar, Prabhakar V. Gulgunje, Bradley A. Newcomb, Kishor Gupta, Han Gi Chae, Yaodong Liu

5d. PROJECT NUMBER

5e. TASK NUMBER

5f. WORK UNIT NUMBER

7. PERFORMING ORGANIZATION NAME(S) AND ADDRESS(ES)
Georgia Institute of Technology
School of Materials Science and Engineering
801 Ferst Dr. NW, MRDC-1
Atlanta, GA 30332-0295

8. PERFORMING ORGANIZATION REPORT NUMBER

9. SPONSORING/MONITORING AGENCY NAME(S) AND ADDRESS(ES)
Air Force Office of Scientific Research
Dr. Joycelyn Harrison
875 N. Randolph St.
Arlington, VA 22203

10. SPONSOR/MONITOR'S ACRONYM(S)
AFOSR

11. SPONSOR/MONITOR'S REPORT NUMBER(S)

12. DISTRIBUTION/AVAILABILITY STATEMENT
This technical report is approved for public release with unlimited distribution

13. SUPPLEMENTARY NOTES

14. ABSTRACT
The density of currently produced polyacrylonitrile based carbon fibers is around 1.8 g/cc. It will be of great benefit to reduce this density so that high-performance structures made from such fibers can be lighter than those made from the solid carbon fibers. With the goal to produce high-strength and high-modulus carbon fibers with densities in the range of 0.9-1.3 g/cc, polyacrylonitrile (PAN) based precursor fibers were produced with a honeycomb structure. Using dry jet wet spinning method, honeycomb precursor fibers were manufactured that consisted of PAN as the sea component and poly(methyl methacrylate) as the islands component. Subsequently, the precursor fibers were stabilized and carbonized to produce hollow carbon fibers. Resulting carbon fibers possessed the estimated density in the range of 1.1 to 1.2 g/cc with tensile modulus in number of trials in the range of 300 to 368 GPa. By comparison, modulus of IM7 fiber with a density of about 1.78 g/cc is 276 GPa. Thus the specific modulus of the hollow carbon fiber can be more than 50% higher than that of state of the art PAN based carbon fiber such as IM7.

15. SUBJECT TERMS
Polyacrylonitrile (PAN), Carbon fiber, honey-comb structure, low density carbon fiber, islands-in-a-sea bi-component fiber

16. SECURITY CLASSIFICATION OF:			17. LIMITATION OF ABSTRACT	18. NUMBER OF PAGES	19a. NAME OF RESPONSIBLE PERSON
a. REPORT	b. ABSTRACT	c. THIS PAGE			Satish Kumar
U	U	U	UU		19b. TELEPHONE NUMBER *(Include area code)* 404-894-7550

TABLE of CONTENTS

Executive Summary

Gel spun PAN and PAN/CNT based carbon fibers with honey-comb cross-section

The density of currently produced polyacrylonitrile based carbon fibers is around 1.8 g/cm^3. It will be of great benefit to reduce this density so that the high-performance structures made from such fibers can be lighter than those made from the solid carbon fibers. With the goal to produce high-strength and high-modulus carbon fibers with densities in the range of 0.9-1.3 g/cm^3, polyacrylonitrile (PAN) based precursor fibers were produced with a honeycomb structure. Using dry jet wet spinning method, honeycomb precursor fibers were manufactured that consisted of PAN as the sea component and poly(methyl methacrylate) as the islands component. Subsequently, the precursor fibers were stabilized and carbonized to produce hollow carbon fibers. Resulting carbon fibers possessed the estimated density in the range of 1.1 to 1.2 g/cm^3 with tensile modulus in number of trials in the range of 300 to 368 GPa. By comparison, modulus of IM7 fiber with a density of about 1.78 g/cm^3 is 276 GPa. Thus the specific modulus of the hollow carbon fiber can be more than 50% higher than that of state of the art PAN based carbon fiber such as IM7. In addition, a number of other studies on structure, processing, and properties of polymer/CNT composite films and fibers were also conducted. Results of these studies are well documented in the many archival publications and two completed Ph.D. theses. These publications and thesis are listed below. Amongst the key additional findings include nano composite fibers with thermal conductivity in the range of 2 – 15 W/m/k. Details of the unpublished work of the honey-comb fiber are included with this report.

Published papers acknowledging AFOSR support:

1. Y. Liu, H. G. Chae, and S. Kumar, "Gel spun carbon nanotube/Polyacrylonitrile composite fibers: Part I – Effect of carbon nanotube on stabilization", *Carbon*, **49**, 4466-4476 (2011). Doi:10.1016/j.carbon.2011.06.043
2. Y. Liu, H. G. Chae, and S. Kumar, "Gel spun carbon nanotube/Polyacrylonitrile composite fibers: Part II – Stabilization reaction kinetics and effect of gas environment", *Carbon*, **49**, 4477- 4486 (2011). Doi:10.1016/j.carbon.2011.06.042
3. Y. Liu, H. G. Chae, and S. Kumar, "Gel spun carbon nanotube/Polyacrylonitrile composite fibers: Part III – Effect of stabilization conditions on the resulting carbon fiber", *Carbon*, **49**, 4487-4496 (2011). Doi:10.1016/j.carbon.2011.06.045

4. M. L. Minus, H. G. Chae, S. Kumar, "Polyethylene Crystallization Nucleated by Carbon Nanotubes under Shear" *ACS Applied Materials and Interfaces.***4**, 326-330 (2012). Doi: 10.1021/am2013757.

5. J. Moon, K. Weaver, B. Feng, H. G. Chae, S. Kumar, J-B.Baek, G. P. Peterson, "Thermal Conductivity Measurement of Individual Poly(ether ketone)/Carbon Nanotube Fibers Using a Steady-State dc Thermal Bridge Method", *Review of Scientific Instruments*, **83**, 016103 (2012). Doi: 10.1063/1.3676650

6. S. Basu-Dutt, M. L. Minus, R. Jain, D. Nepal, S. Kumar, "Chemistry of Carbon Nanotubes for Everyone", *J. Chemical Education*, **89**, 221-229 (2012). Doi:10.1021/ed1005163.

7. E. N. J. Ford, M. L. Minus, T. Liu, J. I. Choi, S. S. Jang, S. Kumar, "Influence of Single Wall Carbon Nanotubes on the Preferential Alignment of Molecular Moieties in PVA Fibers", *Macromolecular Chemistry and Physics*. **213**, 617-626 (2012). Doi: 10.1002/macp.201100534

8. Y. Liu, S. Kumar, "Recent Progress in Fabrication, Structure, and Properties of Carbon Fibers", *Polymer Reviews*, **52,** 234-258 (2012). DOI: 10.1080/15583724.2012.705410.

9. Y. Liu, Y. H. Choi, H. G. Chae, P. Gulgunje, S. Kumar, "Temperature Dependent Tensile Behavior of Gel-spun Polyacrylonitrile and Polyacrylonitrile/Carbon Nanotube Composite Fibers", *Polymer*, **54**, 4003-4009 (2013). http://dx.doi.org/10.1016/j.polymer.2013.05.051

10. A. T. Chien, P. V. Gulgunje, H. G. Chae, A. Joshi, J. Moon, B. Feng, G. P. Peterson, and S. Kumar, "Functional polymer–polymer/carbon nanotube bi-component fibers", *Polymer*,**54**, 6210-6217 (2013). http://dx.doi.org/10.1016/j.polymer.2013.08.061

11. R. Jain, H. G. Chae, and S. Kumar, "Polyacrylonitrile/Carbon Nanofiber Nanocomposite Fibers", *Composites Science and Technology*, **88,** 134-141 (2013).

Ph.D. Theses Completed:

1. Yaodong Liu, "Stabilization and carbonization studies of polyacrylonitrile/carbon nanotube composite fibers." Ph.D. Thesis, Georgia Institute of Technology, 2010.

2. Ericka Johnson Ford, "Carbon Nanotubes as Structural Templates within Poly(vinyl alcohol) Composite Fibers", Studies on poly(vinyl alcohol)-carbon nanotube composite fibers", Ph.D. Thesis, Georgia Institute of Technology, 2012.

LOW DENSITY CARBON FIBERS WITH HONEYCOMB STRUCTURE

Prabhakar V. Gulgunje, Bradley A. Newcomb, Kishor Gupta,
Han Gi Chae, Yaodong Liu, Satish Kumar
School of Materials Science and Engineering, Georgia Institute of Technology, 801 Ferst Drive NW, MRDC-1, Atlanta, GA 30332-0295

ABSTRACT

The density of currently produced polyacrylonitrile based carbon fibers is around 1.8 g/cm^3. It will be of great benefit to reduce this density so that the high-performance structures made from such fibers can be lighter than those made from solid carbon fibers. With the goal to produce high-strength and high-modulus carbon fibers with densities in the range of 0.9-1.3 g/cm^3, polyacrylonitrile (PAN) based precursor fibers were produced with a honeycomb structure. Using dry jet wet spinning method, honeycomb precursor fibers were manufactured that consisted of PAN as the sea component and poly(methyl methacrylate) as the islands component. Subsequently, the precursor fibers were stabilized and carbonized to produce hollow carbon fibers. Resulting carbon fibers possessed the estimated density of 1.1 to 1.2 g/cm^3 with tensile modulus of up to 209 N//tex.

1. INTRODUCTION

Among a variety of precursor fibers available for carbon fiber production, polyacrylonitrile (PAN) based precursor fibers are mainstream, particularly for high strength carbon fibers. T300 is considered as the baseline carbon fiber for aerospace applications with balanced composite properties [1]. Its tensile strength is 3.5 GPa and tensile modulus is 230 GPa [2]. The state-of-the-art carbon fiber based on PAN precursors exhibit high tensile strength up to 7 GPa [3], and high tensile modulus up to 600 GPa [4]. Densities of PAN based carbon fibers fall in the range of 1.75 - 2.0 g/cm^3 [5]. As compared to metals and ceramics used for structural applications, carbon fiber composites have much higher specific strength and modulus. Recent commercial examples of the Boeing 787 dreamliner [6] and Airbus A350 [7], that use substantial amount (50 wt% in 787 Dreamliner) of carbon fiber reinforced plastics (CFRP), demonstrate the importance of low density materials in developing high performance structures. Using 50 wt% carbon fiber composites in 787 dreamliner, the Boeing Company claimed at least 20% improvement in fuel

efficiency in 787 than in the airplanes that are of similar size [8]. Reducing the density of carbon fiber from its current value of around 1.8 g/cm^3 will help in making the structures lighter than existing structures made from solid carbon fibers.

Travis et al. [9] reported that composites made from hollow carbon fibers should have improved impact strength than solid carbon fiber based composites because hollow carbon fiber will improve the shock absorption capacity of the composite. Bending stiffness of composites made from hollow fibers is superior to those made from solid fibers [10]. Higher moment of inertia makes hollow carbon fibers less prone to buckling failure than solid fibers of equal cross sectional area [10]. Differences in the structure and morphology of carbon fibers across the fiber cross-section have been widely studied by several researchers, and it is considered to be due to skin-core structure of solid carbon fibers [11,12,13]. Watt et al. [13] ascribed the origin of skin-core structure in carbon fibers to the process of oxygen diffusion during stabilization of precursor fibers.

Methods used to manufacture hollow carbon fibers include co-axial electrospinning and post treatment [14], bi-component sheath-core wet spinning with PAN as the sheath and poly(vinyl alcohol) PVA as the core [15]. Upon carbonization, these precursor fibers led to production of hollow carbon fibers. In yet another instance, bi-component sheath-core geometry was used to produce PAN based precursors fibers to manufacture hollow carbon fibers, wherein dry jet wet spinning was used with PAN as sheath component and poly(methyl methacrylate) (PMMA) as core component [16]. Using a spinneret with C-shaped geometry, hollow precursor fibers were produced from pitch [17] as well as PAN [18,19]. However, C-shaped spinnerets can only be used in the melt spinning processes. Fergusson [20] developed the technology to manufacture hollow polymeric fibers using dry jet wet spinning method. In this process, while dope was flowing through specially designed spinneret, coagulant was injected at the core of the spinneret. Upon subsequent coagulation of the extrudate, hollow core was formed. Using this technique, Travis et al. [9], manufactured hollow PAN precursor fibers and converted them into carbon fiber. The hollow carbon fibers thus manufactured possessed tensile strength and tensile modulus of 0.5 GPa and 249 GPa, respectively. Lee et al. [21], reported manufacture of hollow carbon fibers from PAN based precursors using electrospinning. Styrene-acrylonitrile (SAN) was used as the sacrificial component in the core. The tensile strength of 1.2 GPa and tensile modulus of 60 GPa was obtained in the carbon fibers manufactured by this process.

Islands-in-a-sea geometry has been shown to be useful in the manufacture of polymeric precursor fibers to obtain hollow carbon fibers [22]. If a bicomponent precursor fiber is made in such a way that shell or sea is PAN based and islands are made of a polymer that degrade thermally during stabilization of the precursor fibers, hollow carbon fibers can be manufactured. In the present work, islands-in-a-sea approach was used to manufacture precursor fibers with honeycomb structure. PAN and PMMA were used as sea and islands components, respectively. The structure and properties development in precursor fibers and in resulting hollow carbon fibers is discussed.

2. MATERIALS AND EXPERIMENTAL METHODS

PAN-co-MAA (96/4) with a viscosity average molecular weight of 250,000 g/mol was obtained from Japan Exlan Co. Ltd, Japan. PMMA with a weight average molecular weight of 350,000 g/mol and *N*,*N*-dimethylacetamide (DMAc) was obtained from Sigma Aldrich. Methanol was obtained from VWR International. PAN polymer was dried under vacuum at 90 ºC for 2 days. DMAc was distilled prior to use. PAN solution was prepared with solid concentrations of 14.5 g/100 mL DMAc at ~90 ºC. PMMA solution was prepared at concentration of 32.5 g/100 mL DMAc at ~110 °C.

Bi-component fiber spinning system supplied by Hills Inc. (Melbourne, FL) was used for the manufacture of precursor fibers. The spin pack used was such that the resulting bi-component fibers consisted of 7 islands. Chae et al. [23] reported the schematic of the equipment, and that of the geometry of the resulting islands-in-a-sea fibers. Fiber spinning equipment consisted of two reservoirs, one for the PAN solution to be fed as the sea component (S), and the other for the PMMA solution to be fed as the islands component (I). Flow rate of PAN solution was maintained at 1.275 cc/min and that of PMMA solution was maintained at 0.225 cc/min. Single hole spinneret with 200 μm diameter, and L/D ratio of 5 was used. Spinneret temperature was 80 ºC. Dry jet wet spinning method was used to obtain precursor fibers with air gap of ~5 cm. Methanol was used as the coagulation medium, and was maintained at room temperature. The as-spun fibers were collected at a spin-draw ratio of 3 and kept immersed in methanol for 3 days prior to drawing. The as-spun fibers were drawn in either three or four stages. In the four stage drawing process, room temperature stretching was followed by stretching in a hot glycerol bath

in three stages at 100 ºC, 135 ºC, and 160 ºC. When using a three-stage drawing process, the room temperature stretching was skipped.

Fully drawn fibers were stabilized and carbonized using a batch process in a tube furnace manufactured by Micropyretics Heaters International (Cincinnati, OH). Several trials of stabilization and carbonization were conducted by varying tension and time. The stress applied during stabilization and carbonization was calculated based on precursor fiber diameter. Stabilization was carried out in air in two stages. In the first stage, the fibers were heated from room temperature to 260 ºC at a rate of 5 ºC/min and held isothermally for 60 min. In the second stage, the fibers were heated to either 325 ºC or 305 ºC at 5 ºC/min and held isothermally for 20 min. The temperature of furnace containing stabilized fibers was increased at the rate of 5 ºC/min to the temperature of 1300 ºC and carbonization was conducted for 10 min under argon environment.

Tensile testing of the precursor fibers was done using RSA-III solids analyzer (TA Instruments, Inc.) at a gauge length of 25.4 mm. The strain rate was 1 %/s for the precursor fiber and average of 20 tests is reported. It is to be noted that tensile properties of precursor fibers were calculated based on overall fiber diameter that includes PMMA as islands. Fiber diameters were calculated using the length-weight method. Cross-sectional micrographs of as-spun fibers were obtained using Leica optical microscope. Cross sectional images of drawn precursor fibers and carbon fibers were obtained using scanning electron microscope, Zeiss Ultra 60 FE-SEM. SEM was calibrated using a standard from Ladd Research Industries. To obtain better contrast between area containing sea component and islands component of precursor fibers, PMMA component was dissolved by immersing thin microtome sections of precursor fibers in nitromethane. Tensile testing of honeycomb carbon fiber was also done using RSA-III solids analyzer (TA Instruments, Inc.) at a gauge length of 12 mm and at the strain rate of 0.1 %/s and was not corrected for compliance. Diameter of carbon fiber was calculated from SEM micrographs using image analysis software ImageJ. Wide-angle X-ray diffraction (WAXD) patterns were obtained on multifilament bundles of precursor fibers, and of carbonized fibers on a Rigaku Micromax-002 diffractometer (operated at 45 kV, 65 mA, λ=0.1542 nm). The diffraction patterns were analyzed using AreaMax V. 1.00 and MDI Jade 6.1. Orientation of the precursor fiber (f_{PAN}) was determined from the azimuthal scan of diffractions (200, 110) corresponding to $2\theta = 16.7º$, while the crystal size (X_c) was determined from the equatorial scan

of same peak using the Scherrer equation with K=0.9 [24]. Orientation of carbon fibers (f_c) was determined from the azimuthal scan at $2\theta = 25^{o}$. Crystal sizes, $L_{(002)}$ and $L_{(10)}$, in carbon fibers were determined using the Scherrer equation. Raman Spectroscopy was performed using a confocal Raman microscope (Alpha-Witek) with a 514 nm laser operated at 3 mW and a 100X objective. Raman spectra were obtained in 300 nm step size across the cross-section of the honeycomb carbon fibers. Cross sections of carbon fiber samples were prepared by mounting a single filament on a copper 3-post TEM grid (Omniprobe) and curing in epoxy (Gatan). The carbon fiber was then thinned using focused ion beam (FIB) milling at 30 kV and polishing at 5 kV using FEI NOVA Nanolab 200 FIB/SEM.

3. RESULTS AND DISCUSSION

The cross sectional images of as-spun fibers show the distribution of PMMA islands in PAN based matrix in Figure 1. It can be seen that overall fiber shape is circular. Also, the islands are fairly uniformly distributed in the sea. As-spun fibers were drawn in multiple stages as described in the experimental section. The drawing conditions are provided in Table 1. SEM images of drawn fiber cross sections are shown in Figure 2.

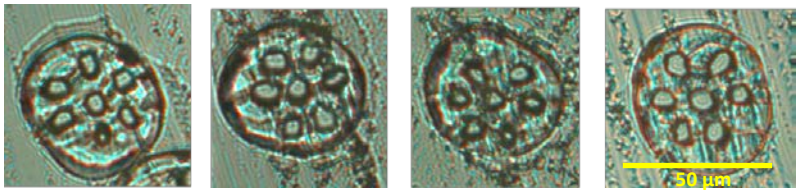

Figure 1 Optical micrographs of honeycomb precursor fiber

Table 1 Drawing conditions of precursor fibers

Fiber	Draw ratio at room temperature stretching	Hot draw ratio (HDR) (100 ºC X135 ºC X160 ºC)	Total draw ratio (TDR)
A	1.4	1.5X1.5X1.7	16
B	--	2.6X1.5X1.6	18

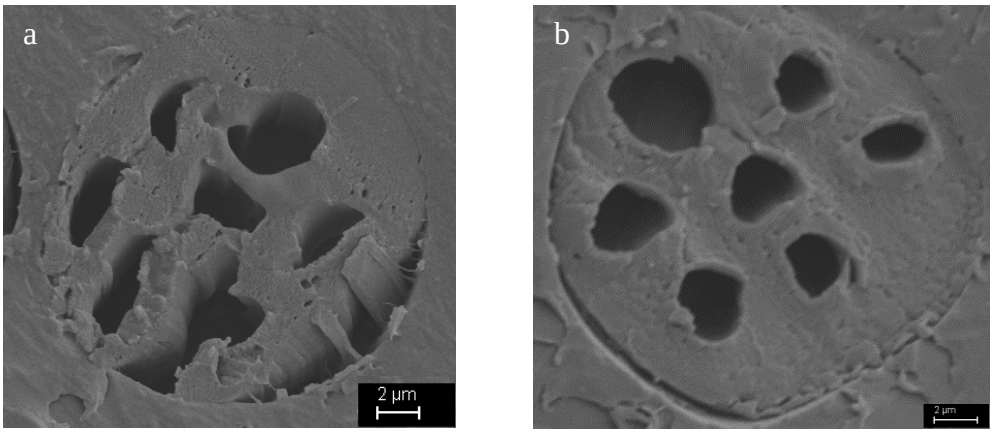

Figure 2. Cross-sectional images of drawn precursor fibers a) Fiber A of Table 1, b) Fiber B of Table 1.

Figure 2a shows that a fiber that was drawn at room temperature followed by 3 stages of hot drawing possess substantial wall breakages, and results in unsatisfactory fiber geometry to convert precursor into successful carbon fiber. Figure 2b shows that the fiber hot drawn in three stages without room temperature stretching possessed improved fiber geometry as compared to the fiber processed through room temperature drawing route. The maximum draw ratio that could be achieved in present study was 18. Due to better cross sectional geometry and intact walls of fiber B of Table 1 than fiber A of Table 1, fiber B was tested for tensile properties. Fiber B was stabilized and carbonized.

Table 2. Tensile properties and structural parameters of precursor fiber B of Table 1

Diameter (µm)	Tensile properties			WAXD	
	Strength (GPa)	Modulus (GPa)	Elongation at break (%)	f_{PAN}	Crystal size (nm)
16.3	0.4 ± 0.03	10.2 ± 1.0	7.3 ±0.4	0.86	9.5

*: Values in parenthesis are the standard deviations of respective properties.

Tensile properties of the precursor fiber B (Table 1) are listed in Table 2. Properties of this precursor fiber are compared with those of single component PAN based precursor fibers spun under comparable process conditions. Tensile properties of honeycomb precursor fibers are poorer than those of single component PAN fibers. Lower tensile properties of honeycomb precursor fibers are partly due to lower drawability of these fibers than single component PAN

fibers, and partly due to the fact that honeycomb precursor fiber properties are based on overall fiber diameter that consists PMMA in the islands.

Stabilization and carbonization conditions for precursor fiber B are listed in Table 3. Also listed in Table 3 are the tensile properties of hollow carbon fibers based on the effective fiber diameter, which is calculated from the solid area of the fiber. For comparison, tensile properties of commercial PAN based solid carbon fiber T300 [2] are also listed in Table 3. Figure 3 shows the cross sectional image of hollow carbon fiber based on honeycomb structure and that of the solid carbon fiber, T300. The tensile modulus of hollow carbon fiber is up to 60% higher than that of T300. Higher tension during stabilization resulted in increased tensile modulus (Trial 2 vs Trial 1). Void fraction in hollow carbon fiber of Figure 3a was 0.375. Assuming the density of carbonized sea component to be similar to that of T300, i.e. 1.76 g/cm^3, estimated density of hollow carbon fiber of Figure 3a is 1.1 g/cm^3. By optimizing the process conditions, carbon fibers with tensile modulus as high as 209 N/tex were obtained. Based on the overall diameter of the carbon fiber, this is a modulus of 244 GPa and based on the equivalent solid carbon fiber diameter, this will be a modulus of 368 GPa.

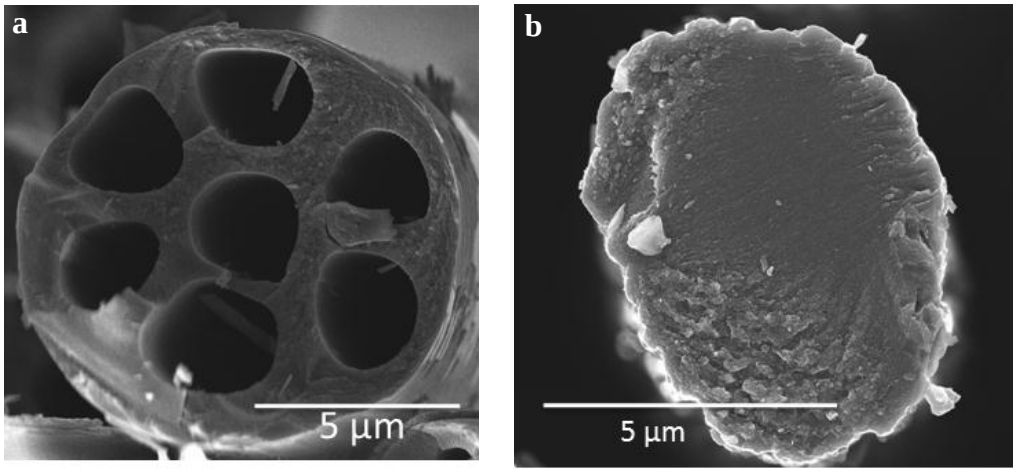

Figure 3 Cross sections of carbon fibers (a) Hollow carbon fiber with honeycomb structure; (b) T300.

Table 3 Stabilization and carbonization conditions and properties of hollow carbon fibers

Trial #	Applied stress* (MPa)	Stabilization-1 temp(ºC)/time (min)	Stabilization-2 temp(ºC)/time (min)	Carbonization temp(ºC)/time (min)	Effective Diameter (µm)	Tensile Strength (GPa)	Tensile Modulus (GPa)	Elongation to break (%)
1	13.9	260/60	325/20	1275/10	8.3 ± 0.3	2.3 ± 0.8	267 ± 96	0.9 ± 0.3
2	24.9/12.8	260/60	325/20	1275/10	9.6 ± 0.3	2.4 ± 0.5	342 ± 28	0.7 ± 0.1
3	27/13.9	260/60	325/20	1275/10	10.1 ± 0.3	2.1 ± 0.5	322 ± 25	0.6 ± 0.1
4	24.9/12.8	260/60	305/20	1275/10	9.3 ± 0.3	2.4 ± 0.6	368 ± 58	0.7
T300					7	3.5	230	1.5

* In the case of two stress values for a given trial, stress corresponding to first value was applied during stabilization, and stress corresponding to the second value was applied during carbonization.

Table 4 Structural parameters of honeycomb carbon fiber and T300

Fiber	f_c	$L_{(002)}$ (nm)	$L_{(10)}$ (nm)	d (nm)
Honeycomb carbon fiber (Trial 1 of Table 3)	0.79	1.3	2.1	0.352
T300	0.77	1.4	2.0	0.349

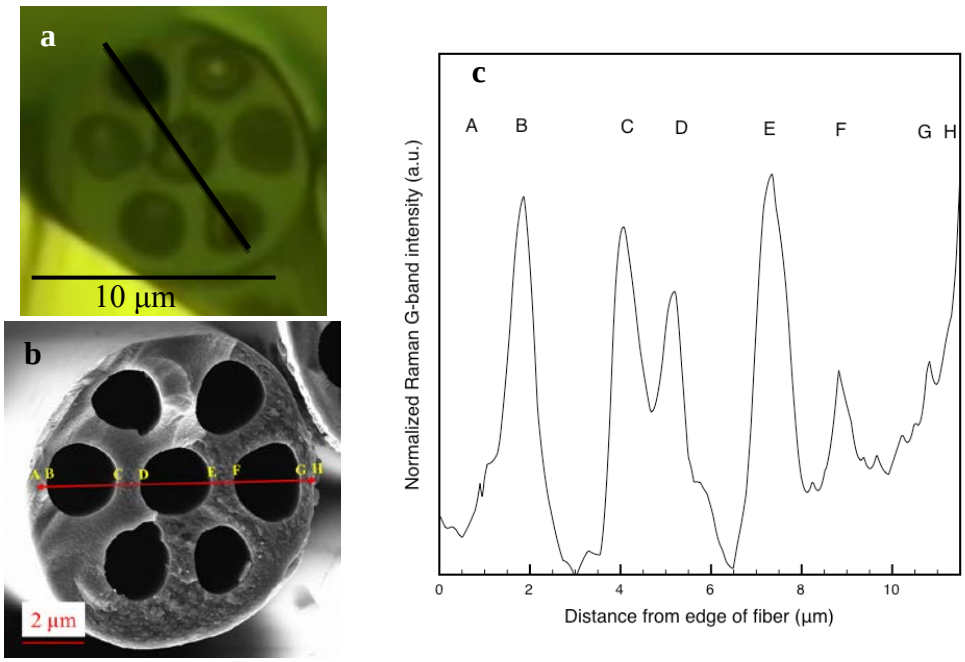

Figure 4 Hollow carbon fiber: (a) optical image and (b) SEM image, (c) Raman spectra across the fiber cross-section

Differences between tensile properties of hollow carbon fibers and T300 can be explained on the basis of fiber structure. WAXD analysis (Table 4) suggests that hollow carbon fibers have slightly higher orientation than T300. Raman spectroscopy was carried out on a hollow carbon fiber shown in Figure 4a, and the Raman spectra at 1590 cm^{-1} wavelength that corresponds to graphitic peak is shown in Figure 4c. Raman spectra was taken along the black line as shown in Figure 4a. The SEM image shown in Figure 4b is of another hollow carbon fiber from the same batch provided for better clarity. It can be seen from Figure 4c that the intensity of graphitic peak is higher at the edges of walls than elsewhere suggesting higher graphitic order at the wall edges, indicating better orientation at these locations, and thus explains enhanced tensile modulus of

hollow carbon fiber than that of T300. Both, precursor fiber manufacture as well as stabilization and carbonization processes contribute to the structural enhancements in the hollow carbon fibers. In addition to shear induced orientation at walls while solution passes through capillary and stress induced orientation due to stretching during precursor fiber drawing, presence of PMMA as islands is expected to cause PAN, at wall edges surrounding PMMA, to experience more shear as compared to PAN in the body, contributing to higher orientation in the regions closer to walls than in the body. During stabilization, complete thermal degradation of PMMA [23] leaves hollow channels inside the fiber. During carbonization, since the wall thickness in hollow fibers is smaller (less than 2 μm) than the diameters of typical solid precursor fibers (~10-12 μm), the total diffusion path length is limited. Lower tensile strength of hollow carbon fibers as compared to T300 is attributed to batch processing.

In Figure 5, the tensile properties of hollow carbon fibers from present work are plotted with other high performance fibers of different densities that are either commercially available or were reported in the literature. Properties of CNT (carbon nanotube) fibers 1, 2, 3 were reported by Koziol et al. [25], and were spun directly from an aerogel of CNTs as they were formed in a reactor. Properties of CNT fiber 4 were reported by Behabtu et al. [26] and were manufactured from CNTs using wet spinning process. Properties of Toray hollow CF were reported by Ishida et al. [15], and were prepared from bi-component fibers using sheath core geometry with PAN as the sheath and PVA as the core components. Properties of commercial fibers, Spectra® 1000 [27], Kevlar® 49 [28], Zylon® [29], T300 [2], IM10 [30], M60J [31], YS-95A [32] were obtained from the data sheets of these fibers from the respective manufacturer. Tensile properties of commercial fibers are typically measured at 25.4 mm gauge length. Properties of T1000GB were reported by Naito et al. [33] at 25 mm gauge length. It is to be noted that the gauge length for the tensile properties measurement reported for CNT fibers 1 and 2 were 6 mm, for CNT fibers 3 and 4 were 20 mm, and for hollow carbon fibers reported in the current work was 12 mm. As can be seen from Figure 5, the low density carbon fiber from the present work falls in the lower range of densities for various high performance fibers. Except the pitch based carbon fibers (K13D and YS-95A) that possess densities above 2 g/cm^3, and PAN based carbon fiber (M60J) that possesses density close to 2 g/cm^3, the specific tensile modulus of the current low density carbon fiber is the highest amongst all high performance fibers.

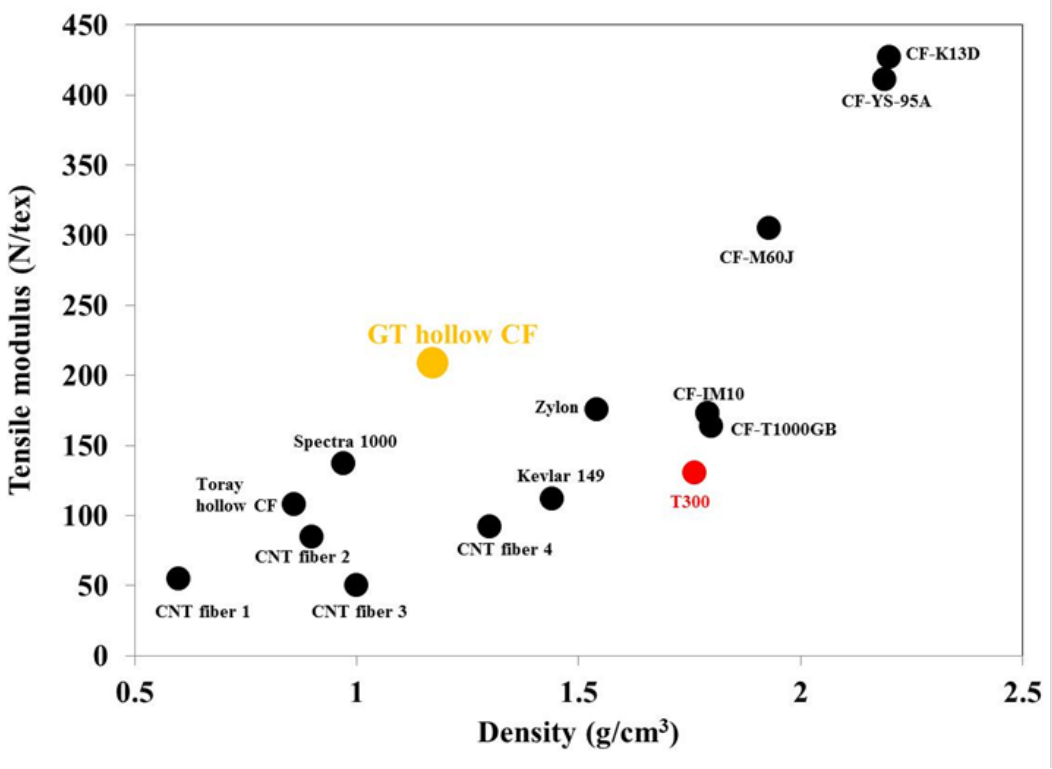

Figure 5. Tensile modulus of carbon fibers as a function of fiber density. GT hollow CF is the low density carbon fiber (Trial 4 of Table 3) from the current study.

Since carbon fiber reinforced plastics (CFRP) are used extensively to develop advanced structures, compressive properties of fibers and resulting composites are also important. Table 5 lists the tensile and compressive properties of commercially available carbon fibers and their unidirectional composites. As per the manufacturers' datasheets of commercial carbon fibers, all the composites made contained 60 vol% fibers in epoxy matrix. Fiber compressive strength may be dependent on fiber structure as well as fiber geometry. Kumar et al. [34] reported that compressive strength of carbon fibers correlates with the width of the graphitic sheets, the crystallite size perpendicular to fiber axis and crystal anisotropy. Generally, compressive strength decreases with increase in carbon fiber tensile modulus. However, carbon fiber with a given modulus can possess higher compressive strength if it can be obtained with desired (002) orientation with smaller crystallite size [34]. With similar crystallite sizes, degree of intracrystallite disorder, and interlayer spacing (d_{002}) between T300 and T800H, Oya et al. [35] ascribed higher compressive strength of T800H than that of T300 to lower porosity in the former fibers, 16.5% porosity for T800H vs 19.7% for T300, respectively. Porosity in the solid portion

of hollow carbon fibers can be expected to be lower than that in T300. Thus, based on micro-structural considerations, the compressive strength of hollow honeycomb carbon fibers should be comparable to those of the fibers such as T800H.

Table 5 Tensile and compressive properties of commercial carbon fibers and their composites

Fiber	Fiber Diameter (μm)	Tensile properties (GPa)		Compressive Properties (GPa)	
		Strength	Modulus	Strength	Modulus
T300	7	3.5	230	1.8	106
T800H	5	5.5	294	2.3	124
M60J	5	3.9	588	1.0	283

If the composite failure is due to buckling, hollow carbon fibers may be advantageous over solid carbon fibers [9]. Under compressive load, PAN based carbon fibers are known to fail due to buckling [36]. Euler's expression can be used to estimate the critical load ($P_{critical}$) at which column of length L will buckle [9] and is given as follows:

$$P_{critical} = \pi^2 * EI/L^2 \qquad 1$$

where, E is modulus of elasticity and I is the cross-sectional moment of inertia.

Based on the buckling consideration also, a hollow carbon fiber of 7 μm diameter will perform better under compression than the 5 μm diameter fiber such as T800H.

4. CONCLUSIONS

PAN based precursor fibers with islands-in-a-sea geometry consisting of good distribution of seven islands in the sea were successfully manufactured. The best hollow carbon fiber manufactured possessed tensile modulus of 209 N/tex, which is 60% higher than that of the commercial solid carbon fiber T300. Factors contributing to high tensile modulus in hollow carbon fibers were shown to be enhanced orientation as evidenced by WAXD and improved graphitic order at the wall edges as seen from Raman Spectroscopy. Thinner walls in the case of honeycomb based hollow carbon fibers as compared to solid T300 fibers are expected to result in improved tensile strength upon continuous carbonization. Carbon fiber with tensile modulus of up to 209 N/tex is by far the best modulus fiber reported in literature for a material with density of ~ 1.2 g/cm^3. On the empirical basis, it is expected that hollow carbon fibers will possess as

good or better compressive strength as compared to the solid carbon fibers such as T300 and T800H.

5. ACKNOWLEDGEMENTS

Financial support for this work from Boeing Company and the Air Force Office of Scientific Research (FA9550-10-1-0475) is gratefully acknowledged. Dr. Smitha Nair's contributions are gratefully acknowledged.

Notes:

-Results of various spinning and carbonization trials are summarized in appendices 1-19

-Polymer used for sea component in the precursor fiber manufacturing trials listed in appendices 1 to 11 and 13 to 15 was polyacrylonitrile-co-methacrylic acid (PAN-co-MAA) with MW 250,000 g/mol

-Polymer used for sea component in the precursor fiber manufacturing trials listed in appendix 12 was polyacrylonitrile-co-itaconic acid (PAN-co-IA) with MW 513,000 g/mol

APPENDICES

Appendix 1. Honeycomb precursor fiber manufacture with various numbers of islands

Trial	Concentration (g/dL) Sea/ Islands	Spinneret diameter (μm)	Sea / Islands solid ratio	Number of Islands	Spinning / MeOH bath Temperature (°C)	SDR×CDR× HDR	Fiber Diameter (μm)	Tensile strength (GPa)	Tensile modulus (GPa)	Strain to failure (%)
1-1	15/32.5	250	62/38	7	100 / -50	2×1.55×5.26	21.3	0.43±0.03	10.7±0.7	9.7±0.8
1-2				7		3×1.55×6.38	17.6	0.49±0.06	13.5±1.4	9.6±1.0
1-3				37		2×1.55×5.26	22.1	0.47±0.14	13.8±4.1	10.4±1.1
1-4				37		3×1.55×6.25	17.6	0.51±0.13	15.6±3.4	8.3±1.0

The tensile properties of all precursor fibers were measured with PMMA present in the islands.

SDR: spin draw ratio, CDR: draw ratio at room temperature stretching, HDR: hot draw ratio, TDR: total draw ratio.

Trial 1-2

Trial 1-4

Cross sectional fiber geometry

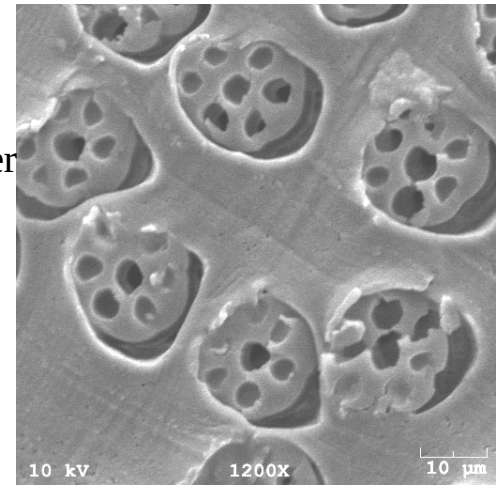

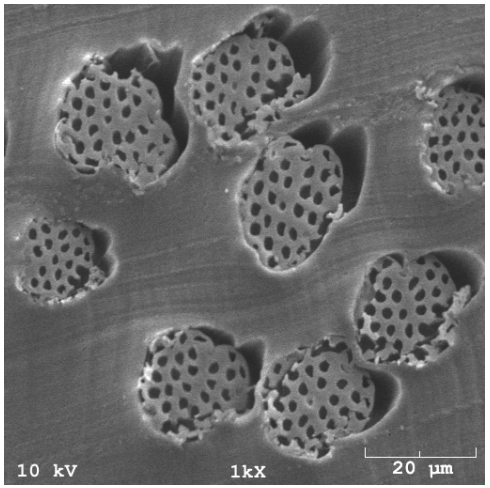

PAN

PMMA

Cross sectional fiber geometry of fiber 1-2 and Schematics

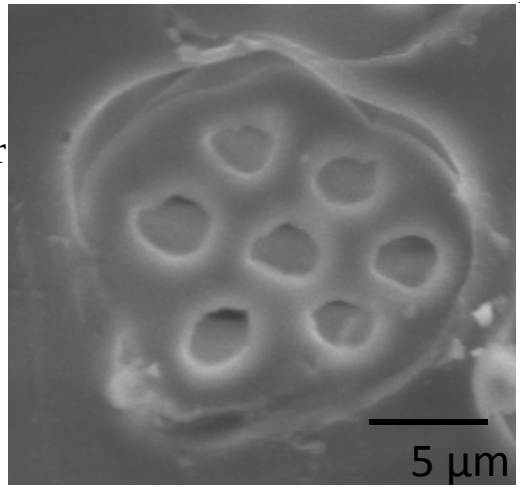

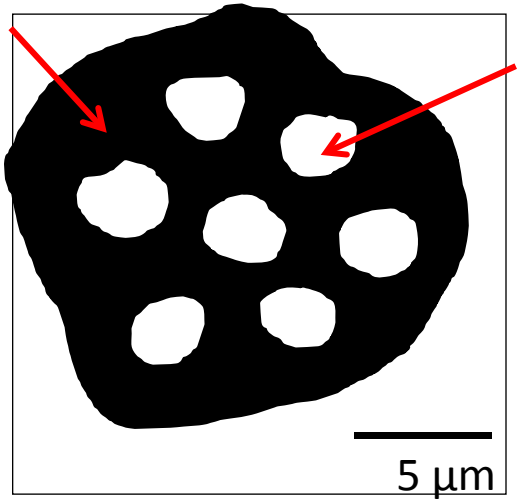

Appendix 2. Honeycomb precursor fiber manufacture using small diameter spinneret (150 µm)

Trial	Concentration (g/dL) Sea/ Islands	Spinneret diameter (µm)	Sea / Islands solid ratio	Number of Islands	Spinning / MeOH bath Temperature (°C)	SDR×CDR× HDR	Fiber Diameter (µm)	Tensile strength (GPa)	Tensile modulus (GPa)	Strain to failure (%)
2	15/30	150	70/30	37	100 / -50	Could not obtain fiber due to uneven extrusion and dripping of polymer solution				
3	15/30	150	60 / 40	37	100 / -50					
4	15/30	150	70/30	7	100 / -50					
5	15/30	150	60 /40	7	100 / -50					

Appendix 3. Honeycomb precursor fiber manufacture with 37 islands

Trial	Concentration (g/dL)	Spinneret diameter (µm)	Sea / Islands solid ratio	Number of Islands	Spinning / MeOH bath Temperature (°C)	SDR×CDR× HDR	Fiber Diameter (µm)	Tensile strength (GPa)	Tensile modulus (GPa)	Strain to failure (%)
	Sea/ Islands									
6	15/30	250	63/37	37	100 / -50	Fibers were not drawn due to non-satisfactory distribution of islands in the sea (Irregular shape fiber)				

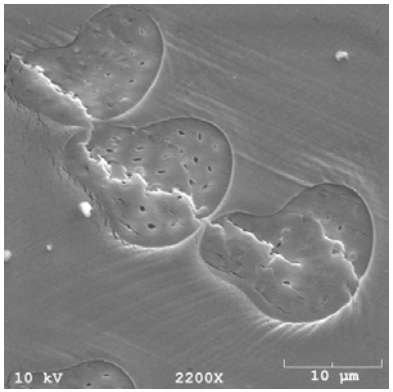

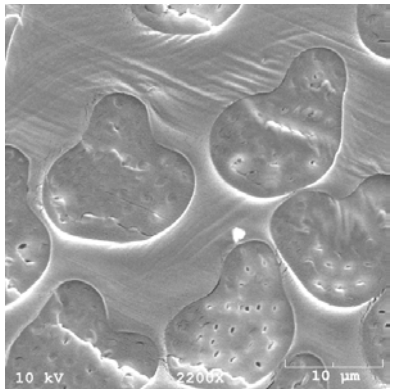

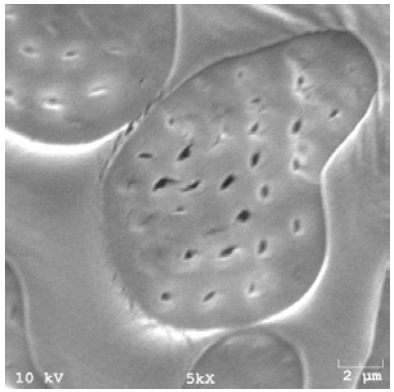

- Fiber cross sectional shape was irregular.
- Due to the better circularity and islands distribution for trial 1-2, further spinning trials were conducted with 7 islands geometry.

Appendix 4. Honeycomb precursor fiber manufacture to increase skin thickness

Trial	Concentration (g/dL) Sea/ Islands	Spinneret diameter (μm)	Sea / Islands solid ratio	Number of Islands	Spinning / MeOH bath Temperature (°C)	SDR×CDR× HDR	Fiber Diameter (μm)	Tensile strength (GPa)	Tensile modulus (GPa)	Strain to failure (%)
7-1	14.5/32.5	250	62/38	7	100 / -50	3×1.55×5	21.6	0.5 ± 0.2	9.9 ± 3.2	8.8 ± 1.1
7-2			67/33	7	100 / -50	3×1.55×5	20.1	0.5 ± 0.2	11.3 ± 4.3	8.8 ± 0.9

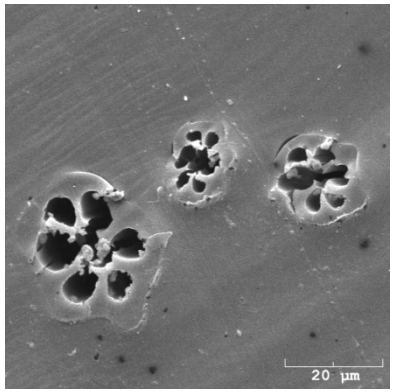

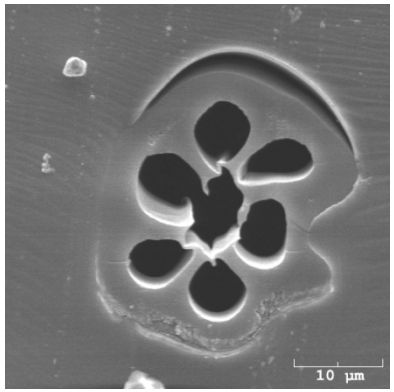

- In trial 1-2, some fibers exhibited that islands component was surrounded by thin skin (sea). Therefore, modified distribution plates were used to increase skin thickness.
- Though skin was thicker in these fibers as compared to the previous trials, wall surrounding the center island was too thin.

Appendix 5. Honeycomb precursor fiber manufacture with distribution plates designed to provide 13 islands and thicker skin

Trial	Concentration (g/dL)	Spinneret diameter (μm)	Sea / Islands solid ratio	Number of Islands	Spinning / MeOH bath Temperature (°C)	SDR×CDR× HDR	Fiber Diameter (μm)	Tensile strength (GPa)	Tensile modulus (GPa)	Strain to failure (%)
	Sea/ Islands									
8	15/30	200	63/37	13	100 / -50	3×1.55×4.9	15.8	0.5 ± 0.03	12.4 ± 0.4	7.5 ± 0.4

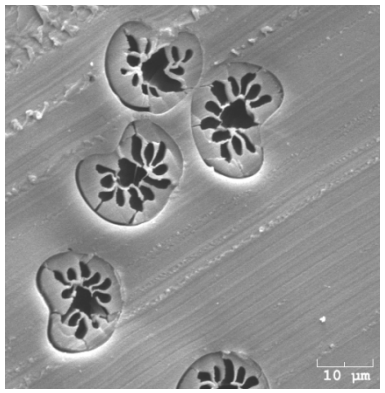

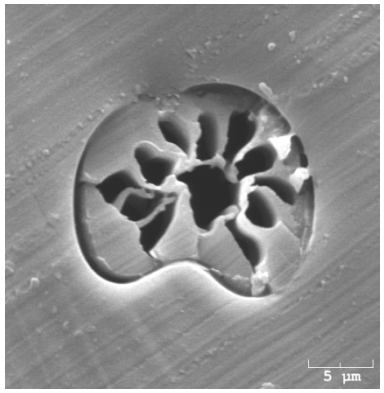

- Thicker skin of precursor fiber was obtained, but inner wall surrounding center island was very thin.
- Only 12 islands were observed, which may be due to merging of two islands.
- Cross sectional shape of the fiber was not circular.

Appendix 6. Reproducibility of trial 1-2

Trial	Concentration (g/dL)	Spinneret diameter (μm)	Sea / Islands solid ratio	Number of Islands	Spinning / MeOH bath Temperature (°C)	SDR×CDR× HDR	Fiber Diameter (μm)	Tensile strength (GPa)	Tensile modulus (GPa)	Strain to failure (%)
	Sea/ Islands									
9	14.5/ 32.5	250	62/39	7	100 / -50	3×1.55×4.5	21.2	0.4 ± 0.1	12.3 ± 0.2	5.2 ± 1.2

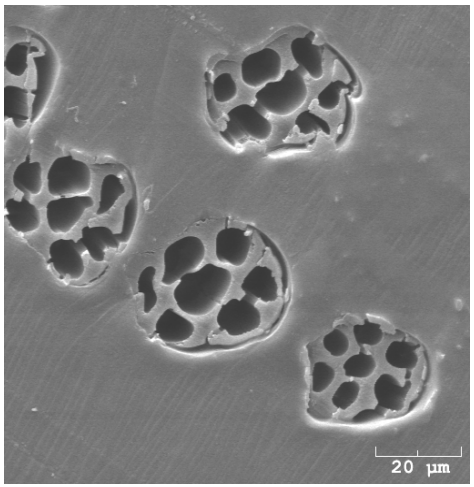

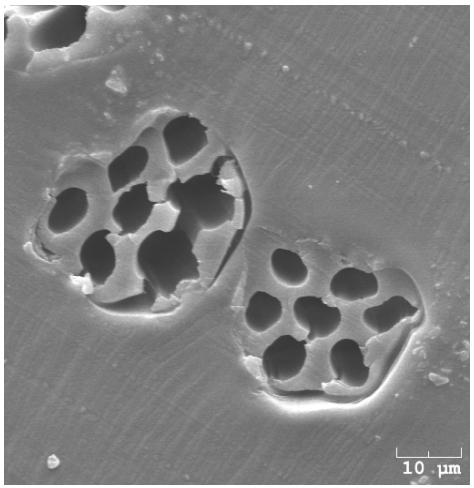

- Overall fiber shape and islands distribution similar as in trial 1-2.
- Better distribution of islands in the fibers as compared to trials 6 to 8, but noticeable wall breakage was present.

Appendix 7. Honeycomb precursor fiber manufacture to obtain fibers with circular cross-sectional shape

Trial	Concentration (g/dL) Sea/ Islands	Spinneret diameter (μm)	Sea / Islands solid ratio	Number of Islands	Spinning / MeOH bath Temperature (°C)	SDR×CDR× HDR	Fiber Diameter (μm)	Tensile strength (GPa)	Tensile modulus (GPa)	Strain to failure (%)
10	14.5/32.5	200	75 / 25	7	100 / -50	3×1.25×6.1	15.4	0.6 ± 0.1	12.9 ± 1.5	7.7 ± 0.8
11	14.5/32.5	200	75 / 25	7	80 / RT	3×1.35×6.5	17.6	0.6 ± 0.1	17.7 ± 1.7	6.4 ± 2.1

Trial 10

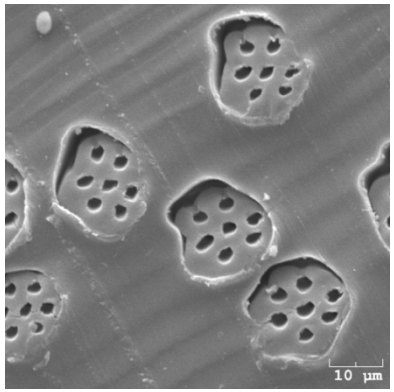

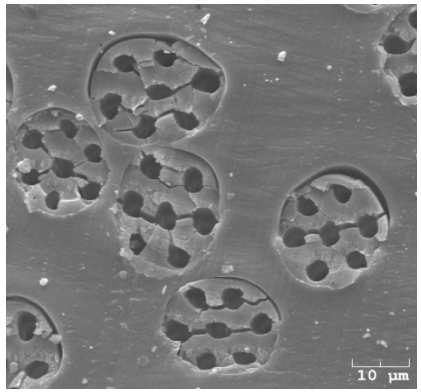

Trial 11

- In trial 11, circular fibers with improved islands distribution were obtained.
- However, wall breakage was still present in the drawn precursor fibers.

Appendix 8: Honeycomb precursor fiber manufacture with PAN/CNT as sea component (0.5 wt% XO122UA)

Trial	Concentration (g/dL)	Spinneret diameter (µm)	Sea / Islands solid ratio	Number of Islands	Spinning / MeOH bath Temperature (°C)	SDR×CDR×HDR	Fiber Diameter (µm)	Tensile strength (GPa)	Tensile modulus (GPa)	Strain to failure (%)
	Sea/ Islands									
12	14/33	200	75/25	7	80 / RT	Not drawn due to non-satisfactory distribution of islands in the sea.				

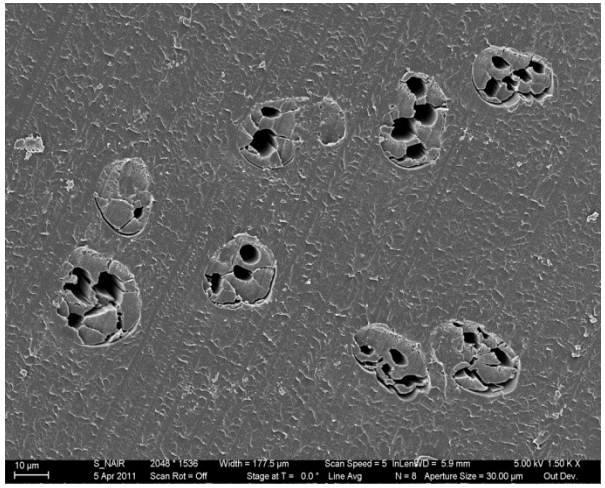

- PMMA solution was degassed to remove air bubbles. However during degassing, solvent evaporated leading to increased viscosity of the PMMA solution and inhomogeneity. Therefore, non-uniform flow of PMMA might have led to irregular islands distribution in the fiber cross section.

Appendix 9: Reproducibility of trial 11

Trial	Concentration (g/dL)	Spinneret diameter (µm)	Sea / Islands solid ratio	Number of Islands	Spinning / MeOH bath Temperature (°C)	SDR×CDR× HDR	Fiber Diameter (µm)	Tensile strength (GPa)	Tensile modulus (GPa)	Strain to failure (%)
	Sea/ Islands									
13	14.5/32.5	200	75/25	7	80 / RT	Fiber was not drawn since further spinning trials were planned to increase skin thickness				

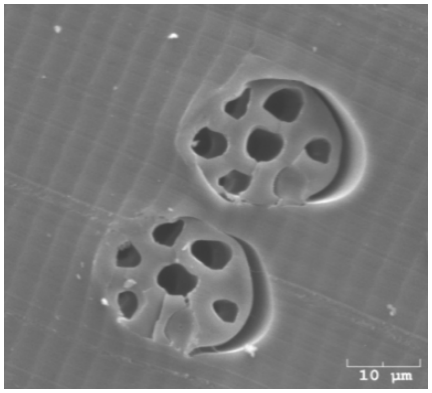

- Cross-sectional geometry obtained was close to that of trial 11.
- To increase the skin thickness, further trials were conducted after obtaining necessary distribution plates from Hills, Inc.

Appendix 10: Honeycomb precursor fiber manufacture with varying skin thicknesses

Trial	Concentration (g/dL) Sea/ Islands	Spinneret diameter (µm)	Sea / Islands solid ratio	Number of Islands	Spinning / MeOH bath Temperature (°C)	SDR×CDR× HDR	Fiber Diameter (µm)	Tensile strength (GPa)	Tensile modulus (GPa)	Strain to failure (%)
14	14.5/32.5	200	80/20	7	80 / RT	Not drawn due to non-satisfactory fiber geometry (Different trials were attempted to obtain different skin thickness by changing distribution plates)				
15	14.5/32.5	200	75/25	7	80 / RT					
16	14.5/32.5	200	75/25	7	80 / RT					

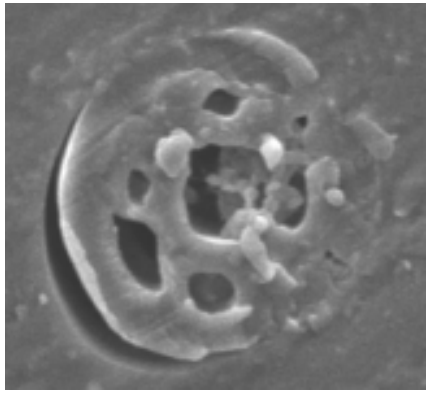

Trial 14

Trial 15

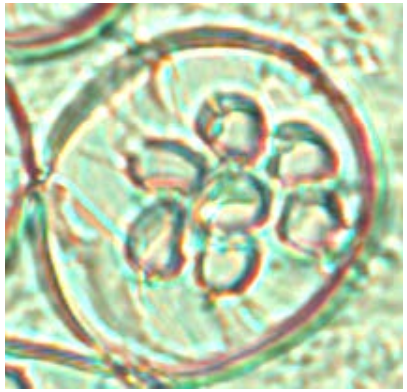

Trial 16

- Under given design of distribution plates, skin was too thick with very little sea component surrounding center island.

Appendix 11: Honeycomb precursor fiber manufacture to obtain fibers with improved geometry

Trial	Concentration (g/dL) Sea/ Islands	Spinneret diameter (µm)	Sea / Islands solid ratio	Number of Islands	Spinning / MeOH bath Temperature (°C)	SDR×CDR× HDR	Fiber Diameter (µm)	Tensile strength (GPa)	Tensile modulus (GPa)	Strain to failure (%)
17	14.5/32.5	200	75/25	7	80 / RT	3×none×6	16	0.4 ± 0.03	10.2 ± 1.0	7.3 ± 0.4
						3×1.4×3.8	18	0.4 ± 0.02	11.5 ± 2.6	6.5 ± 0.4

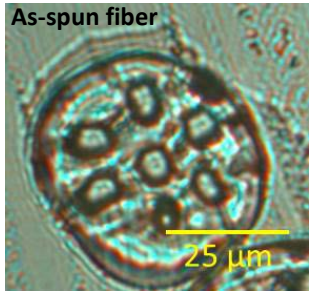

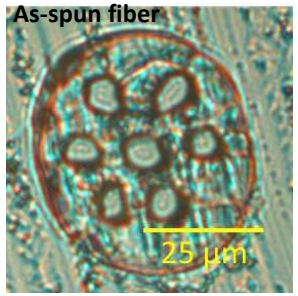

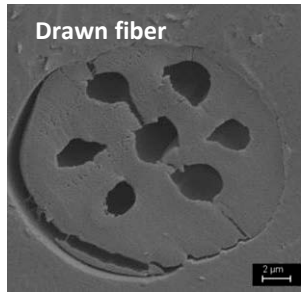

- Repetition of trial 11 was attempted.
- Circular fiber with uniform islands distribution was obtained in the fibers.
- For drawing of this trial, multi-stage drawing was carried out to overcome wall breakage issue.

Appendix 12. Honeycomb precursor fiber manufacture using PAN/CNT as sea component (0.25 wt% XOC231U)

Trial	Concentration (g/dL)	Spinneret diameter (µm)	Sea / Islands solid ratio	Number of Islands	Spinning / MeOH bath Temperature (°C)	SDR×CDR×HDR	Fiber Diameter (µm)	Tensile strength (GPa)	Tensile modulus (GPa)	Strain to failure (%)
	Sea/ Islands									
18	10.5/32.5	200	75/25	7	80 / RT	Fibers were not drawn due to non-satisfactory distribution of islands in the sea				
19	10.5/35	200	75/25	7	80 / RT					
20	10.5/30	200	75/25	7	80 / RT					

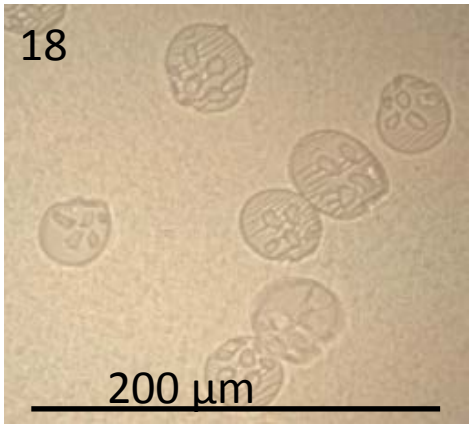

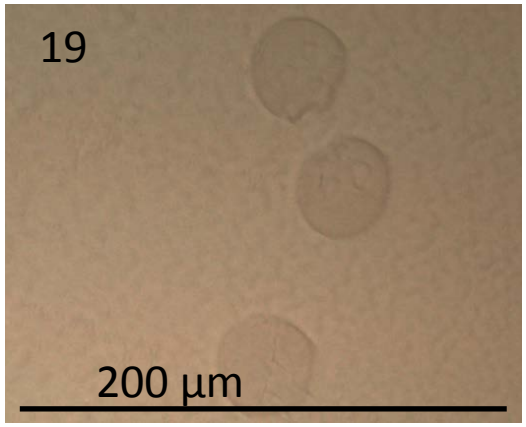

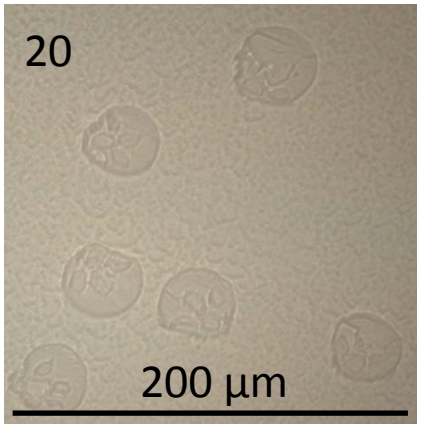

- Islands distribution in all three trials was not uniform
- Cross sections did not show 7 islands in all three cases

Appendix 13: Honeycomb precursor fiber manufacture with PAN/CNT as sea component (0.5 wt% XO122UA)

Trial	Concentration (g/dL) Sea/ Islands	Spinneret diameter (µm)	Sea / Islands solid ratio	Number of Islands	Spinning / MeOH bath Temperature (°C)	SDR×CDR× HDR	Fiber Diameter (µm)	Tensile strength (GPa)	Tensile modulus (GPa)	Strain to failure (%)
21-1	14.5/32.5	200	75/25	7	80 / RT	Fibers were not drawn due to non-satisfactory distribution of islands in the sea				
21-2		200	60/40	7	80 / RT					

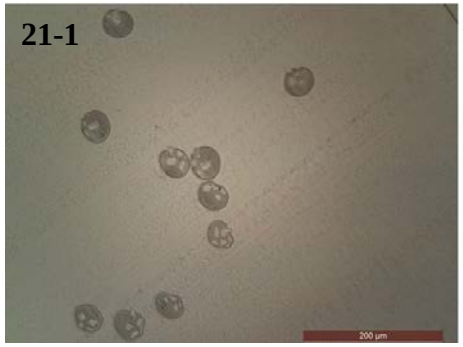

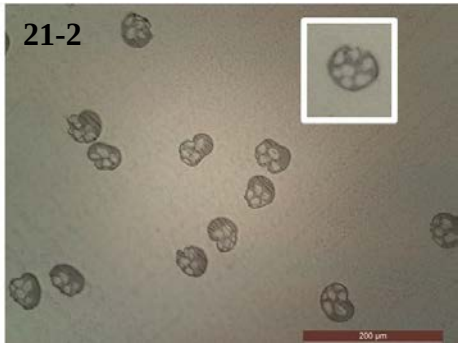

- Islands distribution was poor for both trials, probably due to large viscosity difference between solutions of sea and island components.
- However, trial 21-2 exhibited slightly better islands distribution than trial 21-1.

Appendix 14: Honeycomb precursor fibers with PAN/CNT as the sea component (0.5 wt% XO122UA)

Trial	Concentration (g/dL) Sea/ Islands	Spinneret diameter (µm)	Sea / Islands solid ratio	Number of Islands	Spinning / MeOH bath Temperature (°C)	SDR×CDR× HDR	Fiber Diameter (µm)	Tensile strength (GPa)	Tensile modulus (GPa)	Strain to failure (%)
22-1	14.5/30	200	75/25	7	80 / RT	Fibers were not drawn due to non-satisfactory distribution of islands in the sea				
22-2		200	60/40	7	80 / RT					
22-3		200	50/50	7	80 / RT	3×none×9.0	13.3	0.6 ± 0.06	15.0 ± 1.5	7.2 ± 0.5
22-4						3XnoneX5.1	17.4	0.4 ± 0.02	11.5 ± 0.9	9.2 ± 1.05

Appendix 15. Honeycomb precursor fiber manufacture with PAN/CNT as sea component (1 wt% XO122UA)

Trial	Concentration (g/dL) Sea/Islands	Spinneret diameter (µm)	Sea / Islands solid ratio	Number of Islands	Spinning / MeOH bath Temperature (°C)	SDR×CDR× HDR	Fiber Diameter (µm)	Tensile strength (GPa)	Tensile modulus (GPa)	Strain to failure (%)
23-1	15/28	200	75/25	7	60 / RT	3×none×5.4	17.8	0.3 ± 0.03	11.8 ± 1.3	6.3 ± 1.2
23-2						1.5×none×12	17.1	0.4 ± 0.06	14.7 ± 0.9	5.7 ± 0.8

- Improved cross-sectional shape of precursor fibers was obtained among the composite fiber trials.

Appendix 16. Carbonization of Honeycomb precursor fiber from trial 1

Precursor	Trial No	Applied Stress (MPa)	Stabilization (Temp/time) (°C/min)		Carbonization temp/ Time (°C/min)	Effective Solid Diameter (µm)	Tensile Strength (GPa)	Tensile Modulus (GPa)	Elongation (%)	Void fraction	Theoretical Density of hollow fiber (g/cm^3)
			Step 1	Step 2							
1-2	1	25	255/60	320/20	1100/10	8.2 ± 0.2	1.9 ± 0.4	226 ± 14	0.9 ± 0.3	0.57	0.773

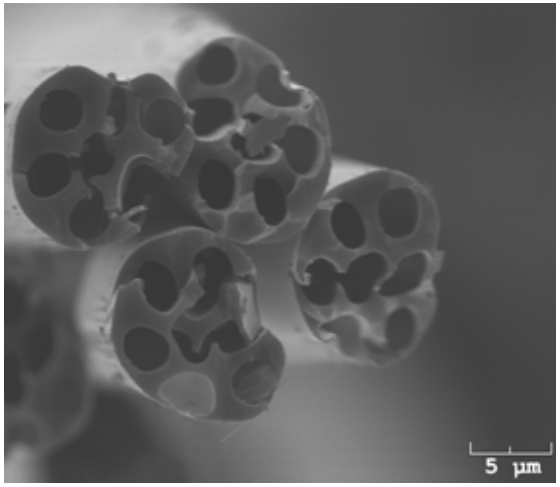

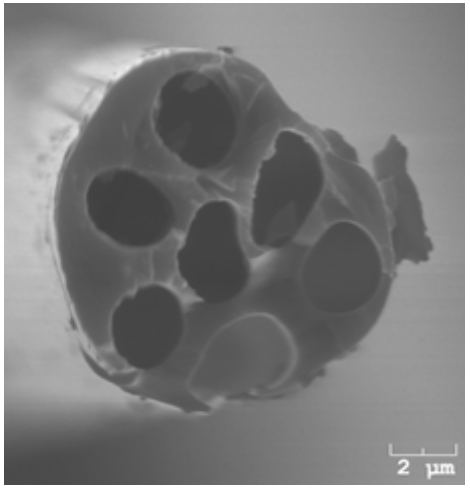

Tensile properties are based on effective solid diameter of the carbon fibers which is calculated from the area of the solid portion in the cross section.

Appendix 17. Carbonization of honeycomb precursor fiber from trial 17

Trial No	Applied Stress (MPa)	Stabilization (Temp/time) (°C/min)		Carbonization temp/ Time (°C/min)	Effective Solid Diameter (µm)	Tensile Strength (GPa)	Tensile Modulus (GPa)	Elongation (%)	Void fraction	Theoretical Density of hollow fiber (g/cm^3)
		Step 1	Step 2							
1	11.6	260/60	325/20	1300/10	Limited number of filament tested					
2	13.9	260/60	325/20	1300/10	Limited number of filament tested					
3	13.9	260/60	325/20	1300/10	8.3 ± 0.3	2.3 ± 0.8	267 ± 96	0.9 ± 0.3	0.4	1.10
4	13.9	260/60	325/7	1300/10	11.8 ± 0.8	1.2 ± 0.4	215 ± 28	0.6 ± 0.2	-	-
5	13.9	260/60	325/38	1300/10	9.8 ± 2.2	1.7 ± 0.4	247 ± 86	0.7 ± 0.2	-	-
6*	24.9/12.8	260/60	325/20	1300/10	9.6 ± 0.3	2.4 ± 0.5	**342 ± 28**	0.7 ± 0.1	-	-
7*	27/13.9	260/60	325/20	1300/10	10.1 ± 0.3	2.1 ± 0.5	**322 ± 25**	0.6 ± 0.1	-	-
8*	24.9/12.8	260/60	305/20	1300/10	9.3 ± 0.5	2.4 ± 0.6	**368 ± 58**	0.7 ± 0.1	0.34	1.16

Tensile properties are based on effective solid diameter of the carbon fibers which is calculated from the area of the solid portion in the cross section.

*: First tension value is the tension applied during stabilization and the second value is the tension applied during carbonization .

Cross sections of carbon fibers

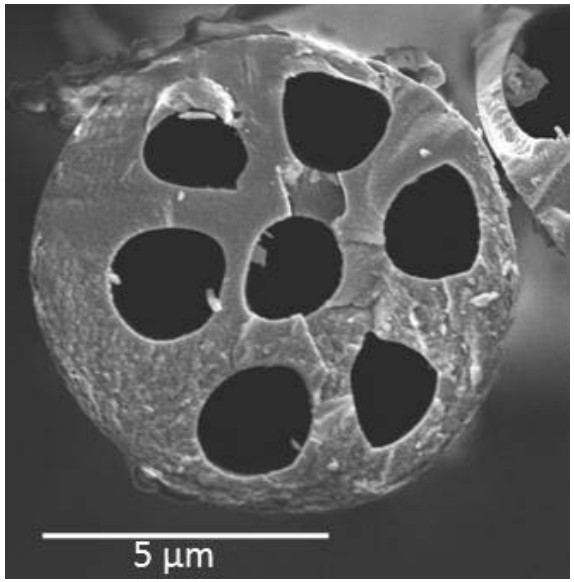

Carbonization trial 17-3

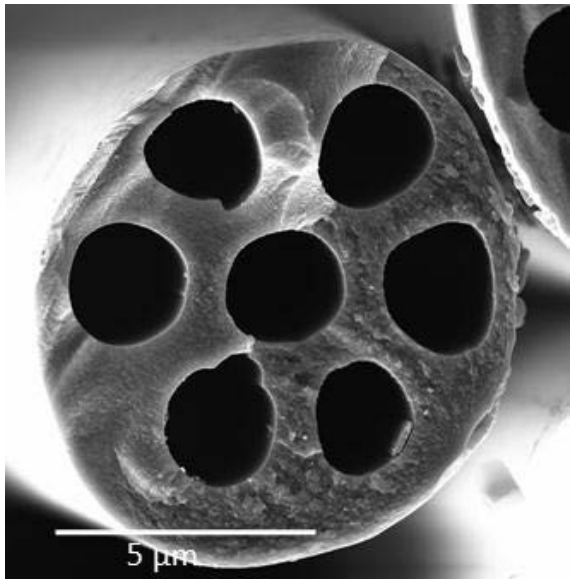

Carbonization trial 17-8

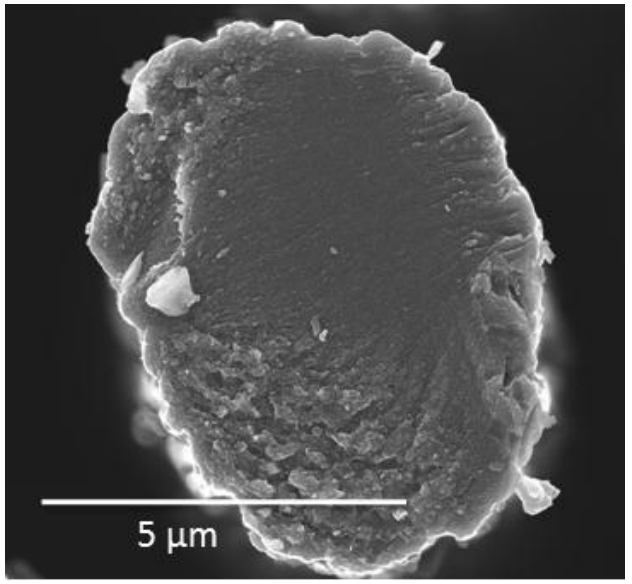

Torayca T-300

- Hollow carbon fibers with honey-comb structure were successfully developed.
- Based on the effective fiber diameter (solid), the tensile modulus exceeds 300 GPa (368 GPa for carbonization trial 8), which is significantly higher than the commercial carbon fiber (T-300, 210 GPa). It should be noted that the tensile modulus of the carbonized honey-comb fiber was not corrected for compliance. Carbon fiber tensile testing was done at 12 mm gauge length.

Appendix 18. Carbonization of PAN/CNT based honeycomb precursor fibers from trial 22

Precursor	Trial No	Applied Stress (MPa)	Stabilization (Temp/time) (°C/min)		Carbonization temp/ Time (°C/min)	Effective Solid Diameter (µm)	Tensile Strength (GPa)	Tensile Modulus (GPa)	Elongation (%)	Void fraction	Theoretical Density of hollow fiber (g/cm^3)
			Step 1	Step 2							
22-3	1*	24.9/13.9	260/60	305/20	1300/5	Broke during carbonization					
22-4	1	24.3	260/60	305/20	1300/5	Broke during carbonization					
	2	19.5	260/60	305/20	1300/5	8.6	0.7 ± 0.3	**300 ± 17**	0.3 ± 0.1	0.61	0.69

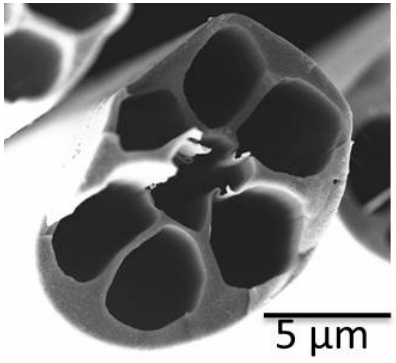

* : First tension value is the tension applied during stabilization and the second value is the tension applied during carbonization.

Appendix 19. Carbonization of PAN/CNT based honeycomb precursor fibers from trial 23

Precursor	Trial No	Applied Stress (MPa)		Stabilization (Temp/time) (°C/min)	Carbonization temp/ Time (°C/min)	Effective Solid Diameter (µm)	Tensile Strength (GPa)	Tensile Modulus (GPa)	Elongation (%)	Void fraction
		Step 1	Step 2							
23-2	30/15.5	260/60	305/20	1300/5	8.6	1.84	222	0.83	0.4	1.06

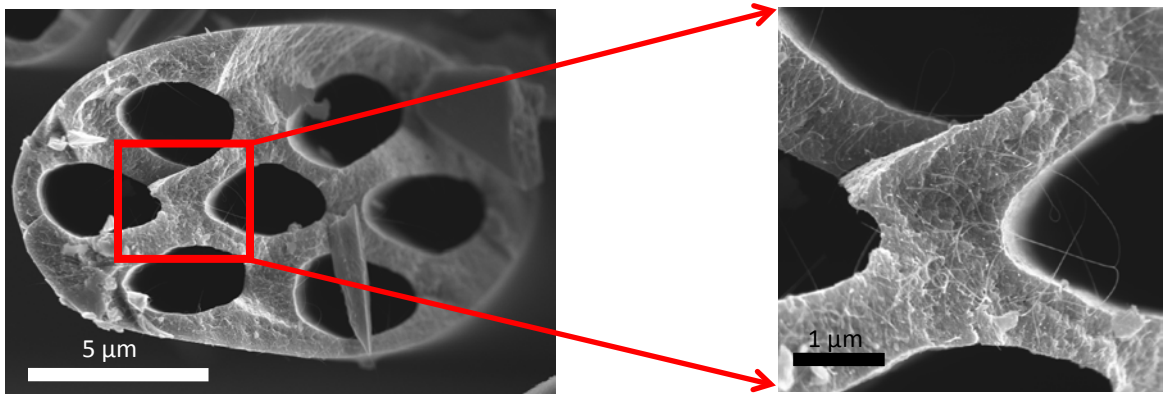

6. REFERENCES

1 http://www.toraycfa.com/standardmodulus.html.

2 http://www.comparts.co.il/files/T300DataSheet.58973619.pdf.

3 http://www.hexcel.com/resources/datasheets/carbon-fiber-data-sheets/im10.pdf.

4 http://www.toraycfa.com/pdfs/M60JDataSheet.pdf.

5 Minus ML, Kumar S, *Journal of Materials* **2005**, 57, p52.

6 http://www.boeing.com/boeing/commercial/787family/programfacts.page.

7 http://www.airbus.com/aircraftfamilies/passengeraircraft/a350xwbfamily/a350-800/.

8 www.boieng.com/boeing/commercial/787family/programfacts.page.

9 S. W. G. Travis, M. Bateson, J. B. Doble, R. E. Palmer, V. Paloumbi, P. T. Curtis, *Proceedings of International Conference on Composite Materials,* Paris, France **2012**, p745.

10 G. Niederstadt, *Zeitschrift für Flugwissenschaften und Weltraumforschung* **1981**, 5, p30.

11 G. Zhou, Y. Liu, L. He, Q. Guo, H. Ye, *Carbon* **2001**, 49, p2883.

12 Y. Huang, R. J. Young, *Carbon* **1995**, 33, p97.

13 W. Watt, W. Johnson, *Proceedings of 3rd Conference on Industrial Carbon and Graphite, Society of Chemical Industries,* London, England **1971**, p147.

14 K. Nayani, H. Katepalli, C. S. Sharma, A. Sharma, S. Patil, R. Venkataraghavan, *Industrial and Engineering Chemistry Research* **2012**, 51, p1761.

15 T. Ishida, T. Higuchi, *Japan Patent P2007-291557A,* **2007**.

16 Y. Liu, H. G. Chae, Y. H. Choi, S. Kumar, Sheath core based hollow carbon fibers, to be published.

17 E. Fitzer, W. Metzler, *Proceedings of the 5th International Carbon Conference, Essen, Germany*, **1992**, p647.

18 C. Li, Y. Tong, L. Xu, X. Yang, Y. Yu, Z. Zhao, *China Patent CN20101108220,* **2011**.

19 E. Fitzer, *European Patent 0433431,* **1991**.

20 J. Ferguson, *US Patent 6143411,* **2000**.

21 B. Lee, K. Park, W. Yu, I. Choi, K. Oh, *18th International Conference on Composite Materials,* Edinburgh, Scotland **2009**.

22 T. Tsotsis, S. Kumar, H. G. Chae, Y. H. Choi, Y. Liu, *Proceedings of the 31st International SAMPE Technical Conference*, Paris, France **2010**.

23 H. G. Chae, Y. H. Choi, M. L. Minus, S. Kumar, *Composites Science and Technology* **2009**, 69, p406.

24 B. D. Cullity, *Elements of X-ray Diffraction*, 2nd ed., Addison Wesley Publishing Company, Reading, MA **1978**, p102.

25 K. Koziol, J. Vilatela, A. Moisala, M. Motta, P. Cunniff, M. Sennett, A. Windle, *Science* **2007**, 318, p1892.

26 N. Behabtu, C. C. Young, D. E. Tsentalovich, O. Kleinerman, X. Wang, A. W. K. Ma, E. A. Bengio, R. F. Waarbeek, J. J. Jong, R. E. Hoogerwerf, S. B. Fairchild, J. B. Ferguson, B. Maruyama, J. Kono, Y. Talmon, Y. Cohen, M. J. Otto, M. Pasquali, *Science* **2013**, 339, p182.

27 http://www51.honeywell.com/sm/afc/common/documents/PP_AFC_Honeywell_spectra_fiber1000_Product_information_sheet.pdf.

28 http://www2.dupont.com/Kevlar/en_US/assets/downloads/KEVLAR_Technical_Guide.pdf.

29 http://www.toyobo-global.com/seihin/kc/pbo/.

30 http://www.hexcel.com/resources/datasheets/carbon-fiber-data-sheets/im10.pdf.

31 http://www.toraycfa.com/pdfs/M60JDataSheet.pdf for M60J.

32 http://www31.ocn.ne.jp/~ngf/english/product/p1.htm.

33 K. Naito, J. M. Yang, Y. Tanaka, Y. Kagawa, *Carbon* **2008**, 46, p189.

34 S. Kumar, D. P. Anderson, A. S. Crasto, *Journal of Materials Science* **1993**, 28, p423.

35 N. Oya, D. J. Johnson, *Carbon* **2001** 39, p635.

36 M. G. Dobb, D. J. Johnson, C. R. Park, *Journal of Materials Science* **1990**, 25, p829.